

## RESEARCH ARTICLE

10.1029/2017JF004361

## Key Points:

- A numerical model helps clarify the extent to which sediment availability influences dune orientation
- This allows linear dunes and barchans to coexist when traditional theory (based solely on wind regime) suggests otherwise
- The model results help us determine sedimentary conditions in cohesionless sand environments where direct sediment sampling is not available

## Correspondence to:

P. Lü,  
lvping@lzb.ac.cn

## Citation:

Lü, P., Dong, Z., & Rozier, O. (2018). The combined effect of sediment availability and wind regime on the morphology of aeolian sand dunes. *Journal of Geophysical Research: Earth Surface*, 123. <https://doi.org/10.1029/2017JF004361>

Received 12 MAY 2017

Accepted 23 OCT 2018

Accepted article online 29 OCT 2018

## The Combined Effect of Sediment Availability and Wind Regime on the Morphology of Aeolian Sand Dunes

Ping Lü<sup>1,2</sup> , Zhibao Dong<sup>1</sup>, and Olivier Rozier<sup>3</sup>

<sup>1</sup>School of Geography and Tourism, Shaanxi Normal University, Xi'an, China, <sup>2</sup>Key Laboratory of Desert and Desertification, Northwest Institute of Eco-Environment and Resources, Chinese Academy of Sciences, Lanzhou, China, <sup>3</sup>Institut de Physique du Globe de Paris, Sorbonne Paris Cité, Université Paris Diderot, Paris, France

**Abstract** Aeolian-driven sand dune orientation is a key parameter that determines dune morphology. Although wind regime, surface condition, and sediment availability all control sand dune formation, researchers have mostly put emphasis on the wind regime. However, research shows that the formation of dune orientation cannot be explained solely on wind because different dune types can form under the same wind regime in a given area. In this study, we investigate the combined effects of wind regime and sediment availability on dune orientation based on numerical simulations. The model clarifies the extent to which sediment availability influences dune orientation as well as the physical mechanisms that allow for the coexistence of different dune types. We found that linear dunes and barchans can coexist when the sediment availability is less than 10% with a localized sand source, and where barchans are situated at the extremity or on the same flank of the linear dunes. When the angle between two dominant winds is greater than 90° and sediment availability is greater than 10%, oblique dunes may occur, and they can evolve from asymmetric barchans. This study offers insight into the potential relationship between dune-forming factors related to the wind regime and the available erodible sediment within a dune system, in view of the fact that such a model would be a valuable tool in ascertaining the causes behind complex dune formation processes.

### 1. Introduction

Sand dunes arise from the accumulation of sediments transported by wind. Accordingly, sand dunes are a dominant geomorphological feature of many deserts and sand-rich landscapes, and their morphology is a key research component in aeolian geomorphology (Bagnold, 1941).

The process and quantitative study of dune geomorphology was pioneered by Bagnold (1941). Subsequently, the field expanded to include field experiments and numerical simulations, which have greatly improved our understanding of dune formation and evolution (Baas & Nield, 2007; Bristow et al., 2000; Courrech du Pont et al., 2014; Hesp, 1981; Jackson & Hunt, 1975; Lancaster, 1995; Livingstone, 1989; Lü et al., 2014, 2016, 2017; McKee, 1979; McKee & Tibbitts, 1964; Rubin & Ikeda, 1990; Tsoar, 1983; Ungar & Haff, 1987; Werner, 1995). Dunes are primarily classified according to shape, slip face number, and origin, and dune evolution is expressed by appraising both sand availability and wind directional variability (Wasson & Hyde, 1983). Hunter et al. (1983) used the angle ( $\alpha$ ) between dune crestlines and the resultant sand transport direction to describe dunes as longitudinal ( $\alpha < 15^\circ$ ), oblique ( $15^\circ < \alpha < 75^\circ$ ), or transverse ( $\alpha \geq 75^\circ$ ). Wasson and Hyde (1983) used the equivalent sand thickness parameter to study the effects of sediment supply on dune type. They found that barchans occur in areas where there is little available sand and virtually unidirectional wind conditions; transverse dunes occur in areas where sand is abundant and wind is moderately variable; longitudinal dunes occur in areas where wind is more variable and there is little available sand; and star dunes occur in areas of abundant sand and maximum wind variability. Barchans and longitudinal dunes are formed under different wind regimes but with almost the same sediment availability. Courrech du Pont et al. (2014) found that a bidirectional flow regime can lead to two different dune orientations according to sediment availability. Dune alignment maximizes dune orthogonality to sand fluxes in conditions with no limit to sand supply, while dunes are aligned with the mean sand transport direction where sand is scarce. Previous research has shown that barchans form under unidirectional wind regimes and limited sediment supplies (Fryberger, 1979; Lancaster, 1995; Tsoar, 2001), whereas linear dunes form under bidirectional wind regimes in cohesionless sand and in landscapes devoid of local roughness elements, such as

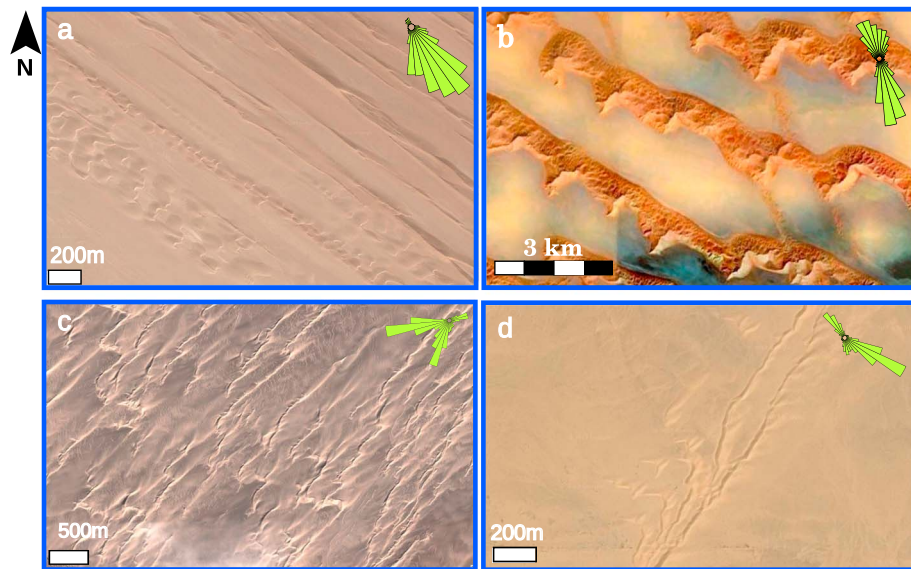


**Figure 1.** The coexistence of linear dunes and barchans (a) at the margins of the Chaerhan Salt Lake desert, China (37.023°N, 93.871°E); (b) the Rub' al-Khali desert, Saudi Arabia (20.85°N, 54.15°E); (c) northern of the Kumtagh desert (40.016°N, 91.812°E); and (d) northern of the Sahara desert (23.470°N, -5.442°E). Insets in (a)–(d) show the local flux roses based on 6-hr winds (above 5-m/s threshold wind speed at 10-m height) from the full period 1979–2016, and the roses show the direction of sand flux. Source: <https://www.google.com/earth/>.

obstructions created by vegetation or bedrock, or alternatively, from unidirectional wind conditions in either cohesive sand or in the lee of obstructions (Rubin & Hesp, 2009).

Thus, this would make it seemingly impossible for both barchans and linear dunes to coexist in the same area. But the Earth observation imagery in Figure 1 show that linear dunes (longitudinal dunes) do coexist with barchans (transverse dunes). Figures 1a–1d illustrate local wind flux conditions supplied by the ERA-Interim data set (Uppala et al., 2005), a global atmospheric reanalysis that since 1979 has provided updated wind speed and orientation data at 10 m above the surface, with a 0.25° horizontal resolution and a 6-hr time resolution. Here we assumed that the threshold wind speed at 10-m height is 5 m/s (Iversen & Rasmussen, 1999). Similarly, high-resolution images from the HiRISE imager onboard NASA's Mars Reconnaissance Orbiter probe also confirm the coexistence of linear dunes and barchans in the northern polar region of Mars (Figure 2). For example, Figure 1a shows that in the Chaerhan Salt Lake desert, China, the coexistence of barchans and linear dunes was caused by the cohesion produced by the widely distributed salts and mud in this area (Rubin & Hesp, 2009), where the unidirectional wind direction derives from the northwest, and Figure 2 reveals linear dune development and barchan ejection in the lee of a topographic obstacle (Lucas et al., 2015). How are we then to explain the conundrum between the coexistence of barchans and linear dunes in Figures 1b–1d?



**Figure 2.** Coexistence of linear dunes and barchans in the northern polar region of Mars (NASA HiRISE image, scene number PSP\_007676\_1385\_RED).

Wind regimes, surface conditions (e.g., vegetation cover), and sediment availability are the three main factors that control the formation and evolution of sand dunes. In areas with little or no vegetation, dune formation depends strongly on wind regime and sediment availability (Baas & Nield, 2007; Wasson & Hyde, 1983), and both factors must be taken into account in studies on the formation and morphology of aeolian dunes; otherwise, modern dune morphology may lead to erroneous interpretations of the evolutionary history of dune environments (Rubin & Hesp, 2009). Gao et al. (2015) studied the effect of sand availability on dune shape and orientation, based on two extremes in sand availability: an erodible sand bed (unlimited sand availability in which to support dune formation, i.e., 100% availability) versus a localized sand source on a nonerodible surface (a fixed nonerodible surface sand source with 7% availability in which to

support dune formation). In the study by Gao et al. (2015), sediment availability ( $\Phi$ ) was controlled by the sediment surface percentage in each cell grid of the model's simulation space, where  $\Phi = 0\%$  represents a nonerodible surface and consequently no sand supply in the cellular space, and  $\Phi = 100\%$  represents unlimited sediment availability, which ensures that bed forms never make contact with nonerodible bedrock at the bottom of the cellular space. However, to date, no studies have been conducted on how variation in sediment availability (from 0% to 100%) affects dune evolution. This has led to a serious gap in our knowledge given that sediment availability varies between 0% and 100% under natural conditions.

The goal of this study was to account for both effects of sediment availability (varying between 0% and 100%) and the wind regime on the morphology and orientation of different dune types. To accomplish this, we conducted numerical simulations based on the Real-Space Cellular Automaton Dune model (ReSCAL).

## 2. The Real-Space Cellular Automaton Dune Model

The ReSCAL (<http://www.ipgp.fr/~rozier/rescal/rescal.html>) combines a traditional cellular automaton model designed for sediment transport with a lattice gas approach for the simulation of turbulent flow over an erodible bed (Chopard & Droz, 1998). This coupled sediment transport and flow dynamics method represents the first implementation of a permanent feedback mechanism between flow and bed form dynamics (Rozier & Narteau, 2014).

The bed form dynamics model is governed by sets of transitions within pairs of nearest-neighbor cells, referred to as "doublets." Each transition is associated with a specific physical process (i.e., erosion, transport, deposition, and the effects of gravity and diffusion) under three different states (fluid, mobile sediment, and immobile sediment; see Figure 2 in Narteau et al., 2009). The lattice gas cellular automaton model is used to compute airflow and quantify the shear stress that it exerts on the bed form as a function of topography. Under specific wind regime effects, physical erosion, transportation, and deposition processes will take place and subsequently cause a change in the bed form (i.e., the topography). Due to topographic changes resulting from shear stress variations in the bed form, flow will also change and will effectively change sediment transport processes (see section 3 in Narteau et al., 2009). Thus, the coupling of the two models is achieved through the effect of shear stress on dune topography. Using lattice gas cellular automaton outputs, we can estimate both velocity field components by averaging the velocity vectors for the fluid particles over space and time. The velocity vector  $\vec{V}$  is expressed in terms of the number of fluid particles, and we used the vector normal  $\vec{n}$  on the topography to calculate shear stress on the bed form ( $\tau_s$ ):

$$\tau_s = \tau_0 \frac{\partial \vec{V}}{\partial \vec{n}} \quad (1)$$

where  $\tau_0$  is the stress scale of the model, expressed in units of  $\text{kg} l_0^{-1} t_0^{-2}$  (where  $l_0$  represents the model's length scale and  $t_0$  represents the time scale of the model). The erosion rate ( $\forall_e$ ) is linearly associated with the shear stress on the bed form ( $\tau_s$ ) according to the following equation:

$$\forall_e = \begin{cases} 0 & \text{for } \tau_s \leq \tau_1 \\ \forall_0 \frac{\tau_s - \tau_1}{\tau_2 - \tau_1} & \text{for } \tau_1 \leq \tau_s \leq \tau_2 \\ \forall_0 & \text{for } \tau_s \geq \tau_2 \end{cases} \quad (2)$$

where  $\forall_0$  is a constant rate,  $\tau_1$  is the initiation threshold of sediment transport, and  $\tau_2$  is a parameter used to adjust the slope of the linear relationship. Excess shear stress ( $\tau_s - \tau_1$ ) is used to calculate the feedback mechanism between the shear stress on the bed form and the topography. In this model, elementary time and length scales  $\{l_0, t_0\}$  are entirely defined with respect to the bed form instability mechanism using the most unstable wavelength and the mean saturated sand flux. Details related to the ReSCAL and its physical parameters are provided in Narteau et al. (2009) and Rozier and Narteau (2014).

Using this model, we can reproduce the extensive natural dune pattern variations that derive from wind regimes and sediment availability. Flow is controlled by the threshold velocity for the inception of motion, wind strength, and the difference ( $\theta$ , an angle in degrees) between two or more wind directions. In this study,

**Table 1**  
*ReSCAL Simulation Parameters*

Variables	Values							
$\theta(^{\circ})$	35	45	60	75	105	120	135	150
$R$	1.0	1.5	2.0	2.5	3.0			
$\Phi(\%)$	7	22	46	64	76	87	100	

we selected a bidirectional wind regime because it has been used to describe the formation of several common dune types (e.g., linear dunes, asymmetric barchans, and transverse dunes).

To study the effect of wind regimes and sediment availability on aeolian dune morphology, we used a rotating cubic lattice to generate a bidirectional wind regime. This model has been used to successfully simulate evolution and formation processes of different dunes, such as star dunes,

transverse dunes, barchans, and linear dunes (Gao et al., 2015; Lü et al., 2014, 2017; Zhang et al., 2010, 2012). The length, width, and height of the simulated 3-D cubic lattice had an order of magnitude of 600, 600, and 120  $l_0$ , respectively, where  $l_0$  is the elementary length scale of the model (see Figure 1 in Rozier & Narteau, 2014). Transition rates of erosion, transport, and deposition (i.e., the rate at which erosion changes to transport or transport changes to deposition) were made constant, and the values were the same as those used by Narteau et al. (2009). In order to study the combined effect of sediment availability and wind regimes on dune development, we set parameters as shown in Table 1.

In Table 1,  $\theta$  and  $R$  represent the different angle and strength ratios between two wind directions, respectively, and  $\Phi$  represents sediment availability. Periodic bidirectional wind regimes can then be fully characterized by the divergence angle  $\theta$  and the transport ratio  $R$  between the two wind directions. The transport ratio is simply the ratio between time for the primary and secondary wind directions over a period of wind reorientation (i.e.,  $R \geq 1$ ). When dunes achieved a steady state in morphology and orientation, the model run was concluded. The following analyses are all based on the steady state of dunes. In this study, dunes took  $t/t_0 \approx 3 \times 10^4$  to  $s t/t_0 \approx 5 \times 10^4$  to achieve steady state.

### 3. Results

Figure 3 shows dune morphology and orientation after achieving steady state under different combinations of sediment availability and wind direction, with wind strength in one direction being twice the strength than in the other direction. In Figure 3, the length of the arrows indicates the proportion between the two wind directions. Clearly, the morphology and the crest orientation of aeolian dunes varied significantly according to the particular combination of wind regime and sediment availability. When the angle between the two wind directions was less than  $90^{\circ}$ , dunes evolved from barchans and barchan chains to transverse dunes as sediment availability increased to greater than 10%. When sediment availability was less than 10% and the angle between the two wind directions was  $75^{\circ}$ , linear dunes formed with barchans oriented in the same direction. However, when the angle decreased to  $60^{\circ}$ , barchans detached from linear dunes and were positioned on the same side or at the terminus of linear dunes, and both linear dunes and barchans moved downwind along the direction of the resultant sand flux. When the angle between two wind directions was greater than  $90^{\circ}$ , most dune types were oblique when sediment availability was greater than 10%. When sediment availability was less than 10%, dune formation was linear with small detached barchans on their sides.

Figure 4 shows simulation results of dune morphology under different wind regimes with less than 10% sediment availability. Dunes can be divided into three types in this study: barchans, linear dunes with detached barchans on their sides, and linear dunes without barchans. This study mainly focused on the second type because of its prevalence and the fact that it has not as yet been well explained by traditional models based solely on wind regimes. When the wind strength ratio was greater than 2.0 and the angle between wind directions was between  $50^{\circ}$  and  $140^{\circ}$ , linear dunes developed along with detached barchans at the downwind terminal end or along the same flank of linear dunes, and some barchans were relatively large compared to those that developed when the wind strength ratio was less than 2.5.

Figure 5 shows the dune types that developed under different wind regimes and sediment availability. The range of conditions suitable for the formation of transverse dunes (labeled "T" in the blue area), linear dunes (labeled "L" in the mauve area), and oblique dunes (labeled "O" in the yellow area) changed in response to changes in the wind strength ratio ( $R$ ), the angle between the two wind directions ( $\theta$ ), and sediment availability ( $\phi$ ). When the strength ratio was 1 (i.e., the two wind directions were of equal strength), the dune type was linear under less than 10% sediment availability and the angle between the two wind directions was greater than  $50^{\circ}$  (Figure 5a). Dune types were barchan (labeled "B"), barchan chains (labeled "C"), and transverse

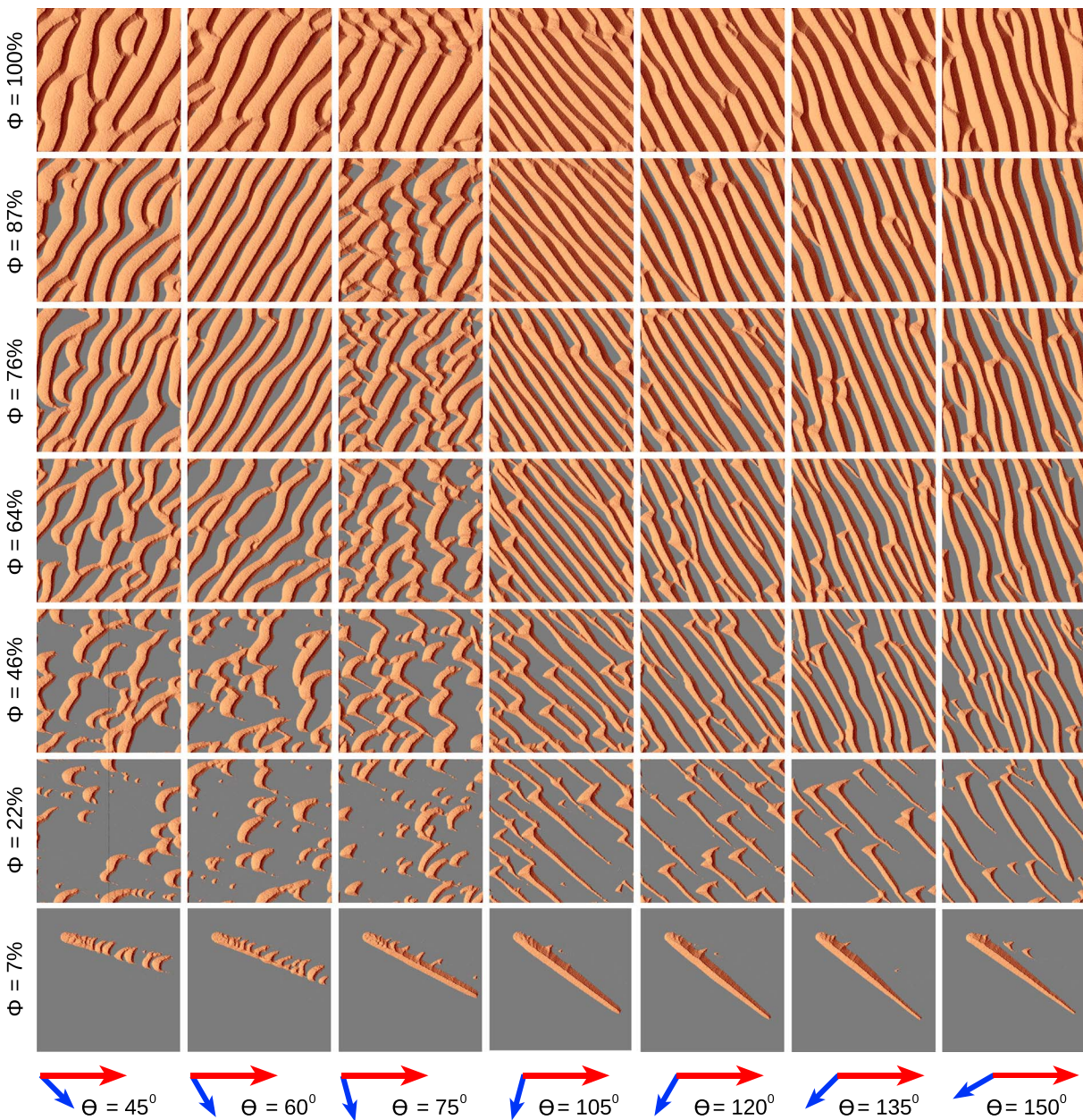


**Figure 3.** Steady state dune morphology in response to changes in sediment availability ( $\Phi$ ) and wind direction ( $\theta$ ) with a wind strength ratio of  $R = 2$ . ReSCAL software was used to produced the images (where  $\theta = 7\%$  represents a fixed sand source with 7% availability, distributed unevenly throughout the domain).

dunes when sediment availability was greater than 10% and the angle between the two wind directions was less than  $90^\circ$ . The dune type then changed to linear as the angle between the two wind directions increased and linear dunes elongated along the direction of the resultant sand flux.

When the strength ratio increased to 1.5, linear dunes and barchans coexisted under less than 10% sediment availability and a  $60^\circ$  wind direction angle, with small detached barchans sometimes forming along with linear dunes. These detached barchans disappeared as the angle between the two wind directions increased, resulting in simple linear dune formations. When the angle between wind directions was  $105^\circ$ , relatively simple linear dunes formed at all levels of sediment availability, but when the angle increased beyond  $105^\circ$ , oblique dunes developed, despite being absent at a strength ratio of 1 (Figure 5a), when all dune types were linear at an angle greater than  $90^\circ$ .

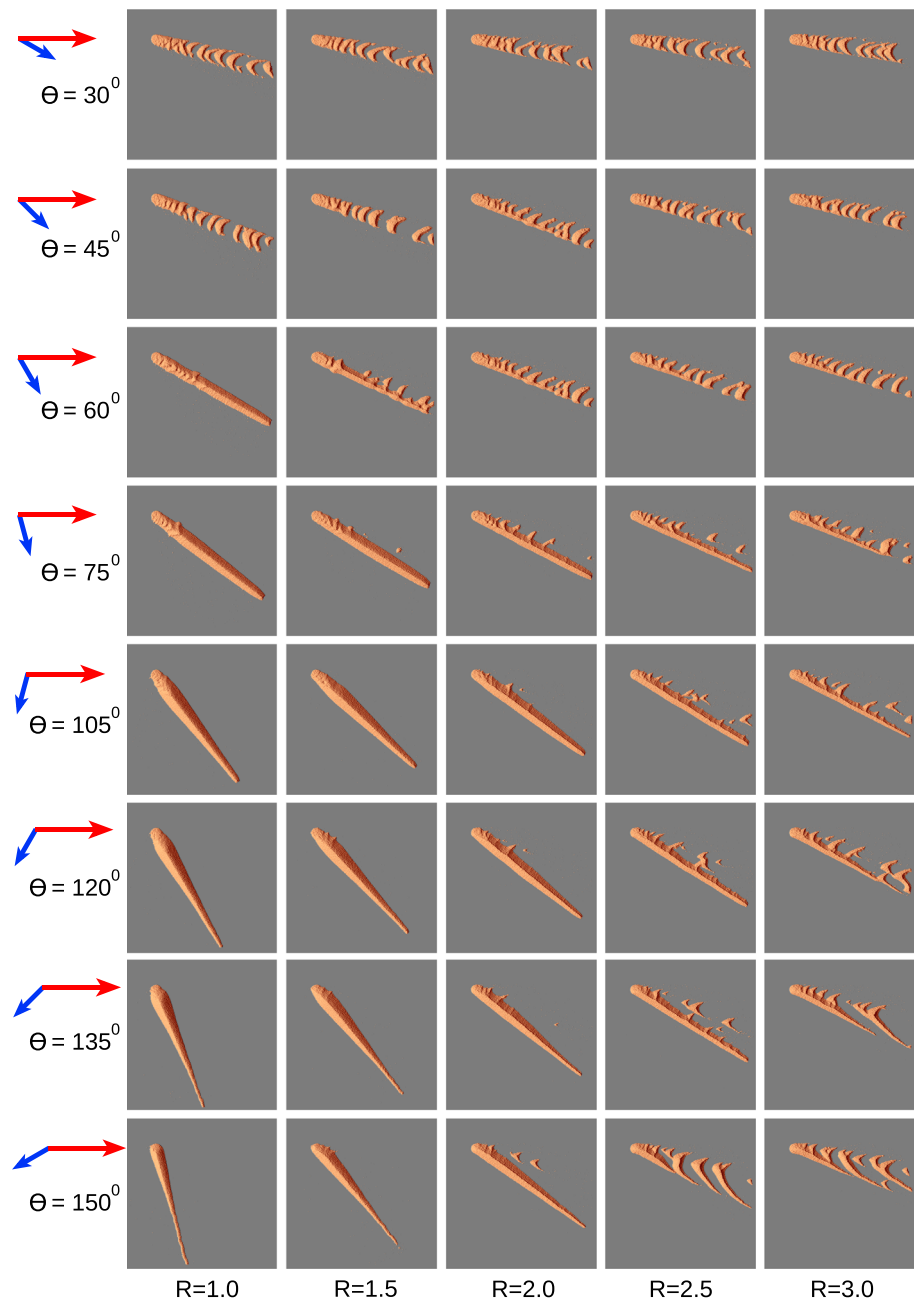


**Figure 4.** Evolution of dune morphology under conditions of limited sediment availability ( $\Phi < 10\%$ ).  $R$  represents the wind strength ratio (i.e., wind strength on the left side of the figure divided by wind strength on the top of the figure).  $\theta$  represents the angle between the two wind directions, and the vector arrows represent a wind direction of  $R = 1.5$ . ReSCAL software was used to produce images.

As seen in Figure 5c, when the wind strength ratio increased to 2, sediment availability was less than 10%, and the angle between wind directions was greater than  $50^\circ$ , all dune types were linear and were accompanied by detached barchans. When sediment availability was greater than 10%, the dune type was barchan or it changed to transverse dunes or barchan chains with increasing sediment availability when the angle between wind directions was less than  $90^\circ$ . When the angle was greater than  $90^\circ$ , the dune type developed into asymmetric barchans under less than 30% sediment availability, but dune type changed to oblique as sediment availability and the angle between wind directions increased. Thus, oblique dunes evolved from asymmetric barchans.

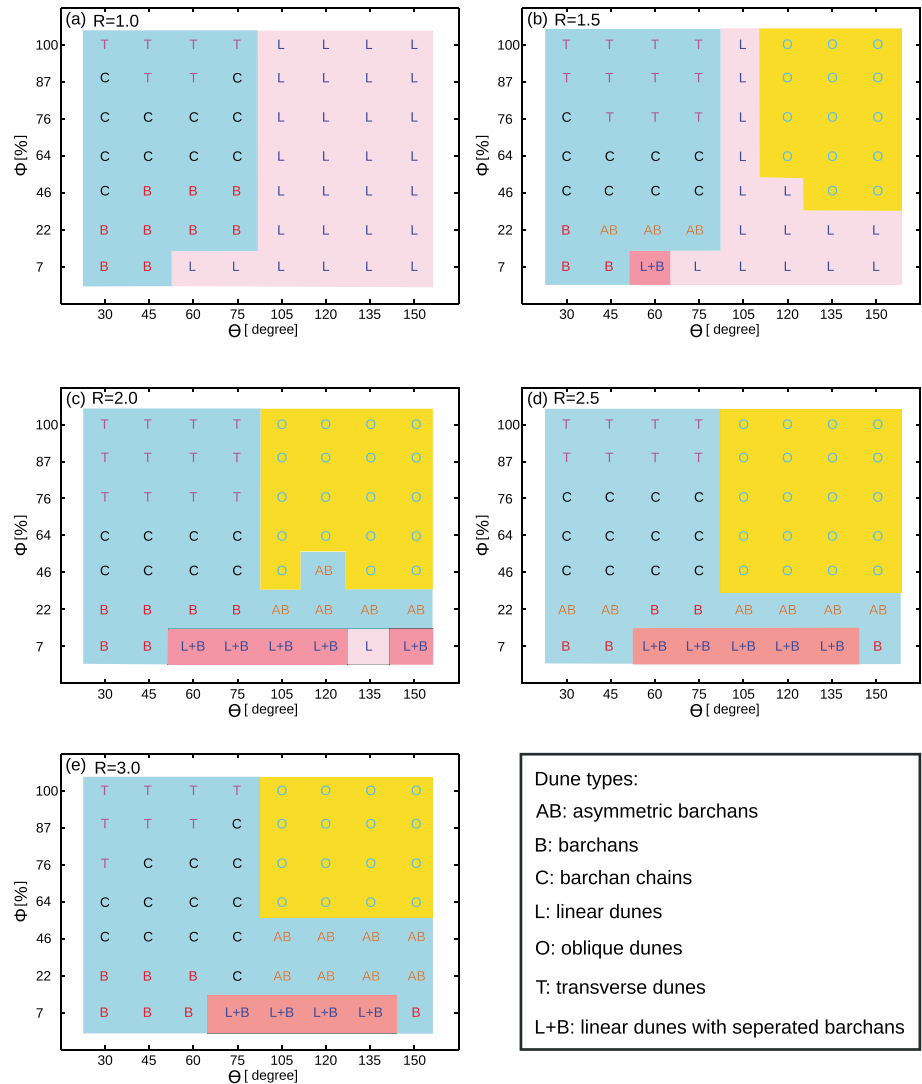


**Figure 5.** The morphological and orientative evolution of steady state dune types under different wind regimes and sediment availability. Dune types were similar for wind strength ratios of 2.5 and 3.0 with less than 10% sediment availability. In both cases, linear dunes and detached barchans coexisted, with barchans sometimes tracking linear dunes and sometimes situated on the same flank as linear dunes.

#### 4. Discussion

Barchans form under unidirectional wind regimes, whereas linear dunes form under bidirectional wind regimes in cohesionless sand and in landscapes free of significant local roughness elements, such as obstructions created by vegetation or bedrock. However, based on Earth observation imagery (<https://www.google.com/earth/>) and NASA's HiRISE image, we found that in some/certain places, linear dunes (longitudinal dunes) coexisted with barchans (transverse dunes). A potential explanation for this phenomenon is that under conditions of unidirectional wind directions and cohesive sand, the downwind accumulation of salts and mud provides cohesion and leads to conditions favorable for coexistence (Rubin & Hesp, 2009). As shown in Figure 1a, in the Chaerhan Salt Lake desert, China, the coexistence of barchans and linear dunes was caused by the cohesion produced by the widely distributed salts and mud in this area (Rubin & Hesp, 2009), where the unidirectional wind direction derives from the northwest (see Figure 1a). A second explanation for the phenomenon is that in the lee of obstructions, linear dunes may develop on the downwind side of the obstacles and eject barchans as showed in Figure 2 (Lucas et al., 2015). Through our numerical

simulation, we found that limited sediment availability derived from point source sediment may lead to the coexistence of linear dunes and barchans within a cohesionless sand environment.

When sediment is limited under a localized sand source conditions, accumulation will form in the lee of the sand source by the effect of wind, and then linear dunes will form and elongate along the resultant sand flux. Separated barchans may occur on the same side of linear dunes, which depends on differences in wind direction and the wind strength ratio.

Dunes in the Rub' al-Khali desert, Saudi Arabia, shown in Figure 1b, formed under a bidirectional wind regime, with the angle and ratio between the two wind directions of approximately  $160^\circ$  and 2.0. Our simulation results (see Figures 4 and 5) show that the coexistence between barchans and linear dunes can occur under this type of wind regime. Therefore, wind conditions in this area favorable to dune coexistence are almost the same as our simulation results. The image shown in Figure 1c is from the northern Kumtag Desert under cohesionless sand and limited sediment availability (Dong et al., 2011). By the flux rose shown in Figure 1c, the primary wind direction is derived from the east, while the secondary wind direction derived from the northeast, where the angle and ratio between the two wind directions were approximately  $60^\circ$  and 1.5–2.0, respectively, which highly corresponded to our simulation results. Based on our simulations (shown in Figure 4), when the angle between two wind directions is  $60^\circ$ , and the strength ratio between them is 1.5 and 2.0, barchans can occur and will be positioned on the same flank as linear dunes. As seen by an increase in flux (see Figure 1d), when the primary wind direction is from the northwest and the secondary wind direction is from the southeast, the angle between them is approximately  $160^\circ$ , and the strength ratio between these two wind directions is nearly 3.0. Based on the simulation results shown in Figure 4, linear dunes with detached barchans can form under a wind regime composed of different angles (at  $150^\circ$ ) and a strength ratio of 3.0. Therefore, the wind regime shown in Figure 1d agrees well with our simulation. Accordingly, wind regimes shown in Figures 1b–1d are roughly the same as our simulation results, illustrating where the coexistence between barchans and linear dunes can occur. Therefore, the morphology of dunes depends greatly on both the wind regime and the sediment availability in cohesionless sandy areas, and this demonstrates the need to account for both factors in studies related to the formation, evolution, and morphology of aeolian dune processes.

However, our study is subject to certain limitations. On the one hand, we should account for the effect of grain size. In this study, we only considered one grain size, which was due to the restrictions of the ReSCAL. Therefore, we plan to further develop the ReSCAL to account for this restriction in future studies. On the other hand, results derived from this study are according to numerical simulation results. It should be noted that numerical simulations can to a certain extent be oversimplified (e.g., only accounting for one grain size and flat surfaces) in order to decrease model complexity and make the model easier to operate, which can result in certain discrepancies between numerical simulations and real-world conditions. However, we plan to conduct field experiments in desert areas where barchans and linear dunes coexist in order to improve our knowledge of aeolian dune geomorphology and subsequently improve the model.

## 5. Conclusions

In this study, we described the combined effects of sediment availability and wind regimes on dune morphology based on numerical simulation results using the ReSCAL software. We found that sediment availability had an important effect on the shape and spatial organization of aeolian dune processes, especially when sediment availability was less than 10% under localized sand sources. When sediment availability was less than 10% of point source concentrations, linear dunes coexisted along with detached barchans. These detached barchans can exist at the terminus of linear dunes or along the same flank of barchans. Barchans, barchan chains, asymmetric barchans, and transverse dunes develop according to variations in sediment availability when the divergence of two wind directions is less than  $90^\circ$ , and oblique dunes develop under the divergence of two wind directions greater than  $90^\circ$ .

Our study offers four significant and novel results. First, we demonstrated the formation and evolution of aeolian dune morphology by accounting for the effect of sediment availability. Second, our results revealed the mechanisms that underlie the coexistence of linear dunes and barchans, and thereby support continued research on the formation and evolution of different dune types. Third, model outcomes presented in this study can help us determine sedimentary conditions in cohesionless sand environments on our as well as

other planets where direct sediment sampling is not available. Fourth, our results illustrate how aeolian geomorphology transpires from interactions between dominant physical processes and the main factors involved in physical processes. By improving our understanding of these processes, we will be better able to describe the evolution of the morphology of modern sand seas on Earth as well as other planetary bodies and draw stronger inferences on their evolutionary history in response to changes in aeolian dune environments.

#### Acknowledgments

We would like to thank three anonymous reviewers for their useful comments on a preliminary version of this manuscript. The data presented in this study are the results of numerical simulations using the Real-Space Cellular Automaton Laboratory (ReSCAL). ReSCAL is a free software available under the GNU General Public License. The source codes can be downloaded from <http://www.ipgp.fr/rescal>. Images in Figure 1 are courtesy of Google Earth, and the image in Figure 2 is courtesy of NASA. We are grateful for the financial support from the National Natural Science Foundation of China (grant 41571008).

#### References

- Baas, A., & Nield, J. (2007). Modelling vegetated dune landscapes. *Geophysical Research Letters*, *34*, L06405. <https://doi.org/10.1029/2006GL029152>
- Bagnold, R. (1941). *The physics of blown sand and desert dunes* (pp. 22–45). London: Methuen.
- Bristow, C., Bailey, S., & Lancaster, N. (2000). The sedimentary structure of linear sand dunes. *Nature*, *406*(6791), 56–59. <https://doi.org/10.1038/35017536>
- Chopard, B., & Droz, M. (1998). Cellular automata modeling of physical systems. In R. A. Meyers (Ed.), *Encyclopedia of complexity and systems science* (Vol. 122, pp. 865–892). New York: Springer.
- Courrech du Pont, S., Narteau, C., & Gao, X. (2014). Two modes for dune orientation. *Geology*, *42*(9), 743–746. <https://doi.org/10.1130/G35657.1>
- Dong, Z., Su, Z., Qian, G., Luo, W., Zhang, Z., & Wu, J. (2011). *Aeolian geomorphology of the Kumtagh desert*. Beijing, China: Science Press.
- Fryberger, S. (1979). Dune forms and wind regime. In E. D. McKee (Ed.), *A study of global sand seas* (pp. 137–160). Washington: U.S. Government Printing Office.
- Gao, X., Narteau, C., Rozier, O., & Courrech du Pont, S. (2015). Phase diagrams of dune shape and orientation depending on sand availability. *Scientific Reports*, *5*(1), 14677. <https://doi.org/10.1038/srep14677>
- Hesp, P. (1981). The formation of shadow dunes. *SEPM Journal of Sedimentary Research*, *51*. <https://doi.org/10.1306/212F7C1B-2B24-11D7-8648000102C1865D>
- Hunter, R., Richmond, B., & Alpha, T. (1983). Storm-controlled oblique dunes of the Oregon coast. *Geological Society of America Bulletin*, *94*(12), 1450–1465. [https://doi.org/10.1130/0016-7606\(1983\)94<1450:SODOTO>2.0.CO;2](https://doi.org/10.1130/0016-7606(1983)94<1450:SODOTO>2.0.CO;2)
- Iversen, J., & Rasmussen, K. (1999). The effect of wind speed and bed slope on sand transport. *Sedimentology*, *46*(4), 723–731. <https://doi.org/10.1046/j.1365-3091.1999.00245.x>
- Jackson, P., & Hunt, J. (1975). Turbulent wind flow over a low hill. *Quarterly Journal of the Royal Meteorological Society*, *101*(430), 929–955. <https://doi.org/10.1002/qj.49710143015>
- Lancaster, N. (1995). *Geomorphology of desert dunes*. London: Routledge.
- Livingstone, I. (1989). Monitoring surface change on a Namib linear dune. *Earth Surface Processes and Landforms*, *18*, 661–664.
- Lü, P., Dong, Z., Narteau, C., & Rozier, O. (2016). Morphodynamic mechanisms for the formation of asymmetric barchans: Improvement of the Bagnold and Tsoar models. *Environment and Earth Science*, *75*, 259.
- Lü, P., Narteau, C., Dong, Z., Rozier, O., & Courrech du Pont, S. (2017). Unravelling raked linear dunes to explain the coexistence of bedforms in complex dunefields. *Nature Communications*, *8*, 14239. <https://doi.org/10.1038/ncomms14239>
- Lü, P., Narteau, C., Dong, Z., Zhang, Z., & Courrech du Pont, S. (2014). Emergence of oblique dunes in a landscape-scale experiment. *Nature Geoscience*, *7*(2), 99–103.
- Lucas, A., Narteau, C., Rodriguez, S., Rozier, O., Callot, Y., Garcia, A., & Courrech du Pont, S. (2015). Sediment flux from the morphodynamics of elongating linear dunes. *Geology*, *43*(11), 1027–1030. <https://doi.org/10.1130/G37101.1>
- McKee, E. (1979). *A study of global sand seas*. Reston, VA: US Geological Survey.
- McKee, E., & Tibbitts, J. (1964). Primary structures of a seif dune and associated deposits in Libya. *Journal of Sedimentary Research*, *34*(1), 5–17.
- Narteau, C., Zhang, D., Rozier, O., & Claudin, P. (2009). Setting the length and time scales of a cellular automaton dune model from the analysis of superimposed bed forms. *Journal of Geophysical Research*, *114*, F03006. <https://doi.org/10.1029/2008JF001127>
- Rozier, O., & Narteau, C. (2014). A real-space cellular automaton laboratory. *Earth Surface Processes and Landforms*, *39*(1), 98–109. <https://doi.org/10.1002/esp.3479>
- Rubin, D., & Hesp, A. (2009). Multiple origins of linear dunes on Earth and Titan. *Nature Geoscience*, *2*(9), 653–658. <https://doi.org/10.1038/ngeo610>
- Rubin, D., & Ikeda, H. (1990). Flume experiments on the alignment of transverse, oblique, and longitudinal dunes in directionally varying flows. *Sedimentology*, *37*(4), 673–684. <https://doi.org/10.1111/j.1365-3091.1990.tb00628.x>
- Tsoar, H. (1983). Dynamic processes acting on a longitudinal (seif) sand dune. *Sedimentology*, *30*(4), 567–578. <https://doi.org/10.1111/j.1365-3091.1983.tb00694.x>
- Tsoar, H. (2001). Types of aeolian sand dunes and their formation. In N. J. Balmforth & A. Provenzale (Eds.), *Geomorphological fluid mechanics* (pp. 403–429). Berlin, Heidelberg: Springer Berlin Heidelberg. [https://doi.org/10.1007/3-540-45670-8\\_17](https://doi.org/10.1007/3-540-45670-8_17)
- Ungar, J., & Haff, P. (1987). Steady state saltation in air. *Sedimentology*, *34*(2), 289–299. <https://doi.org/10.1111/j.1365-3091.1987.tb00778.x>
- Uppala, S., Kallberg, P., Simmons, A., Andrae, U., & Bechtold, V. (2005). The ERA-40 re-analysis. *Quarterly Journal of the Royal Meteorological Society*, *131*(612), 2961–3012. <https://doi.org/10.1256/qj.04.176>
- Wasson, R., & Hyde, R. (1983). Factors determining desert dune types. *Nature*, *304*(5924), 337–339. <https://doi.org/10.1038/304337a0>
- Werner, B. (1995). Eolian dunes: Computer simulations and attractor interpretation. *Geology*, *23*(12), 1107–1110. [https://doi.org/10.1130/0091-7613\(1995\)023<1107:EDCSAA>2.3.CO;2](https://doi.org/10.1130/0091-7613(1995)023<1107:EDCSAA>2.3.CO;2)
- Zhang, D., Narteau, C., & Rozier, O. (2010). Morphodynamics of barchan and transverse dunes using a cellular automaton model. *Journal of Geophysical Research*, *115*, F03041. <https://doi.org/10.1029/2009JF001620>
- Zhang, D., Narteau, C., Rozier, O., & du Pont, S. C. (2012). Morphology and dynamics of star dunes from numerical modelling. *Nature Geoscience*, *5*(7), 463–467. <https://doi.org/10.1038/ngeo1503>